Direct phase-locking of a 8.6-μm quantum cascade laser to a mid-IR optical frequency comb: application to precision spectroscopy of N_2O

Alessio Gambetta,[1,*] Marco Cassinerio,[1] Nicola Coluccelli,[1] Eugenio Fasci,[2] Antonio Castrillo,[2] Livio Gianfrani,[2] Davide Gatti,[1] Marco Marangoni,[1] Paolo Laporta,[1] and Gianluca Galzerano[1]

[1]*Istituto di Fotonica e Nanotecnologie—CNR and Dipartimento di Fisica—Politecnico di Milano, Piazza Leonardo da Vinci 32, Milano 20133, Italy*

[2]*Dipartimento di Matematica e Fisica—Seconda Università di Napoli, Viale Lincoln 5, Caserta 81100, Italy*

**Corresponding author: alessio.gambetta@polimi.it*

Received October 13, 2014; revised December 11, 2014; accepted December 13, 2014; posted December 16, 2014 (Doc. ID 224799); published January 19, 2015

We developed a high-precision spectroscopic system at 8.6 μm based on direct heterodyne detection and phase-locking of a room-temperature quantum-cascade-laser against an harmonic, 250-MHz mid-IR frequency comb obtained by difference-frequency generation. The ~30 dB signal-to-noise ratio of the detected beat-note together with the achieved closed-loop locking bandwidth of ~500 kHz allows for a residual integrated phase noise of 0.78 rad (1 Hz–5 MHz), for an ultimate resolution of ~21 kHz, limited by the measured linewidth of the mid-IR comb. The system was used to perform absolute measurement of line-center frequencies for the rotational components of the ν_2 vibrational band of N_2O, with a relative precision of 3×10^{-10}.

OCIS codes: (140.5965) Semiconductor lasers, quantum cascade; (140.3425) Laser stabilization; (140.7090) Ultrafast lasers; (300.6320) Spectroscopy, high-resolution.

Quantum cascade lasers (QCLs) are proving flexible and robust mid- and far-infrared light sources with CW output powers up to several watts, narrow emission linewidth, and wide tuning range [1,2]. These unique characteristics allow the use of QCLs in a wide variety of applications such as astrophysics and space-science, high-resolution spectroscopy, medical diagnostics, environmental sciences, industry, and homeland security. In particular, in precision spectroscopy a great effort is aimed at further improving the spectral purity while keeping their wide tunability. Among the different stabilization techniques so far demonstrated to control the emission frequency of QCLs [3–6], coherent phase lock to an optical frequency comb is a very simple and effective solution that allows for tuning the optical frequency with absolute precision, as well as narrowing the emission linewidth [7–13]. In the past decade, the advent of optical frequency combs [14] has given a tremendous impact on high-precision spectroscopy due to their capability of down-linking the domain of optical frequencies to that of radiofrequency (RF) standards, paving the way for absolute optical-frequency measurements with unprecedented accuracy and reproducibility [15]. In particular, the synthesis of mid-infrared (mid-IR) optical frequency combs [16] is of primary importance in molecular spectroscopy due to the strong absorption provided by the fundamental roto-vibrational bands and first overtones of many molecules. Among the different approaches pursued so far to generate optical frequency combs in the mid-IR spectral region, the DFG process is very appealing because it provides intrinsic stabilization of the comb, due to the passive cancellation of the offset frequency (f_0) as well as the suppression of common mode noises of pump and signal arms. The result is a narrow-linewidth harmonic comb, with the pulse repetition frequency (f_{rep}) as the only free parameter. This removes the need of further stages in order to detect and lock f_0.

In this Letter, we report on metrological-grade mid-IR spectroscopy based on frequency-comb-assisted distributed-feedback (DFB) QCL, tunable in the wavelength range from 8.56 to 8.63 μm. The QCL laser is phase-locked to a tooth of a DFG mid-IR comb using a beat note generated directly in the mid-IR region without any conversion scheme: the result is a compact spectroscopy system combining the broadband parallel-detection capabilities of a mW-level mid-IR comb to the high-precision performances of a mid-IR narrow-linewidth source. To the best of the authors knowledge, this is the first time that a heterodyne signal between a mid-IR frequency comb and a QCL is detected directly in the 8.6-μm spectral region. This achievement was possible thanks to the hundreds nanowatts comb-mode power level, in the spectral range from 7.8 to 10 μm, of our mid-IR comb [17]. By tuning f_{rep}, the QCL fre-quency is scanned across nitrous oxide (N_2O) transition lines with an ultimate accuracy of a GPS-disciplined Rb frequency standard. Nitrous oxide was selected in this spectroscopic demonstration because this molecule is an important greenhouse gas that plays a fundamental role in the atmospheric radiation balance and to the ozone layer depletion [18]. In addition, N_2O is one of the burning products of the organic fuels in the air. As a consequence, high-resolution spectra of this molecule are of fundamental interest in various applications, like monitoring its concentration in the atmosphere and in the combustion exhaust.

The experimental setup for the high-precision spectroscopy system is shown in Fig. 1. The mid-IR comb synthesis, spanning the 8–14 μm, is based on DFG in a GaSe nonlinear crystal pumped by a dual-branch 250-MHz Er:fiber laser oscillator following the scheme reported in [17]. The main output of the Er:fiber laser provides 1.55-μm 50-fs-long pulses with an average output power of 550 mW, which are used as a pump for the DFG

This is the accepted version of Gambetta A., Cassinerio M., Coluccelli N., Fasci E., Castrillo A., Gianfrani L., Gatti D., Marangoni M., Laporta P., Galzerano G., OPTICS LETTERS, 2015, 40:3, 304-307.
The final publication is available at: http://dx.doi.org/10.1364/OL.40.000304

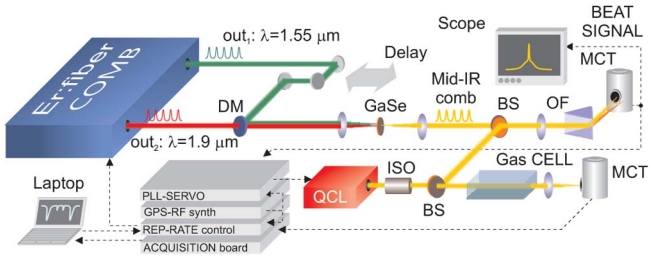

Fig. 1. Experimental setup for absolute N_2O spectroscopy at 8.6 μm. BS, beam splitter; DM, dichroic mirror; ISO, optical isolator; MCT, mercury-cadmium-tellurate detector; OF, optical filter.

process. The second output, coupled to a nonlinear Raman fiber, produces 100-fs-long tunable self-frequency shifted (SFS) solitons in the 1.76–1.93-μm range with an optical power varying from 100 to 250 mW depending on the wavelength, which are used as a signal for DFG. Pump and signal pulses are overlapped in time by means of a delay-stage, combined on a dichroic beam splitter and tightly focused onto a 1-mm-thick GaSe crystal. The mid-IR DFG beam is long-pass filtered and collimated with a plano–convex CaF_2 lens. By changing the Raman soliton wavelength and phase-matching angle, the mid-IR radiation is tuned to a central wavelength of 8.6 μm, with an average output power of 4 mW in an optical bandwidth of 0.8 μm, corresponding to 0.22 μW per comb tooth. The DFB-QCL operates at 20°C (few mK of thermal stability) with a maximum output power of ~10 mW at 8.6 μm and slightly astigmatic beam with $M^2 \sim 1.1$. A low-noise commercial current driver (Wavelength Electronics QCL1500), with a nominal current noise spectral-density of 3 nA/$\sqrt{\text{Hz}}$ and a ~2 MHz modulation bandwidth, has been employed. The QCL and the mid-IR comb beams are superimposed by means of a 50/50 ZnSe beam splitter, filtered by a 0.01-μm-resolution monochromator, and focused onto a 200-MHz bandwidth mercury-cadium-tellurite (MCT) detector with a responsivity of 5.7×10^4 V/W, 50 nV/$\sqrt{\text{Hz}}$ noise floor at a temperature of 77 K and 60-μW saturation power-level.

Figure 2 shows the heterodyne beat notes recorded by an electrical spectrum analyzer, for a 60-μW optical power incident on the detector, which leads to a shot noise level of 46 nV/$\sqrt{\text{Hz}}$. When the QCL operates in free-running, a beat note signal with a SNR ratio as high as 30 dB and a FWHM linewidth of ~1 MHz is observed in a resolution bandwidth of 1 kHz [see Fig. 2(a)]. In order to phase-lock the QCL to the closest mid-IR comb tooth, the beat signal was up-mixed to 336 MHz, frequency divided by a 32 prescaler, and finally compared with a low-noise synthesizer in a fast digital phase-detector. By means of a 1-MHz-bandwidth analog proportional-derivative-integrative (PID) servo, the correction signal is fed back to the QCL driver. In closed-loop operation, a significant narrowing of the beat note linewidth is observed, with a corresponding increase of the SNR larger than 25 dB (1-kHz resolution bandwidth). A maximum SNR of about 60 dB at 1-Hz resolution-bandwidth was obtained, as shown in Fig. 2(b). A ~500 kHz phase-lock control-bandwidth can be inferred from the spectral-shape of the closed-loop beat note signal [Fig. 2(a)]. The phase-lock performance was characterized, in terms

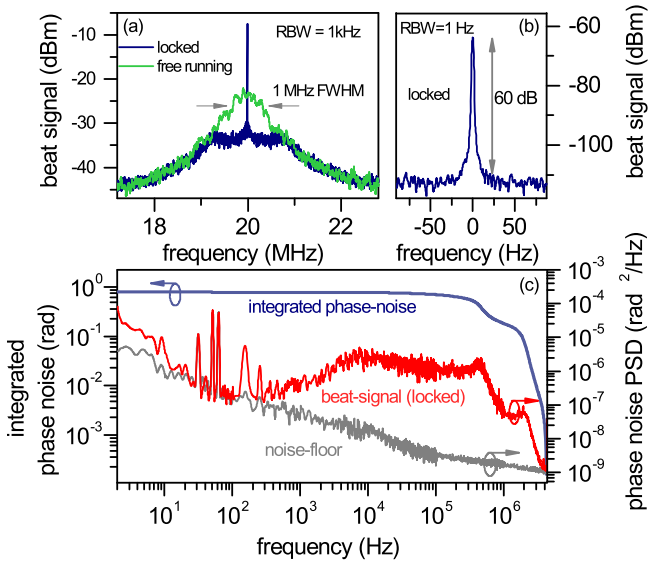

Fig. 2. (a) Beat note signal between the mid-IR comb and the free-running (green curve) and the phase-locked (blue curve) QCL. (b) Phase-locked beat note with higher resolution. (c) Phase noise PSD and integrated phase noise versus integration bandwidth.

of residual phase noise, by measuring the power spectral density (PSD) of the error signal at the output of the phase detector. Figure 2(c) shows the measured phase-noise PSD (right axis) together with the integrated residual phase noise (left axis). A 0.78-rad rms residual phase noise is obtained in the integration bandwidth from 1 Hz to 5 MHz, indicating that more than 54% of the RF power is concentrated in the coherence peak of the beat note [19].

We characterized the frequency-noise properties of the QCL by using the side of a Doppler broadened N_2O line as an optical frequency discriminator and by measuring the frequency-to-intensity converted noise-PSD. The measurement was performed both in slow- and in tight-lock conditions. In order to keep the QCL optical frequency centered on the line-shoulder, the comb f_{rep} was locked to an RF synthesizer referenced to a GPS-disciplined Rb frequency standard. The measured PSDs are shown in Fig. 3 (right axis) together with the RIN contribution and the detector noise floor. In slow-lock conditions the QCL frequency noise is characterized by a flicker, $1/f$, contribution for Fourier frequencies between 2 and 100 kHz, whereas for larger frequencies, it decreases with a $1/f^2$ trend, a result in good agreement with those previously published [6,7,11,20]. Frequencies lower than 2 kHz are within the slow-loop bandwidth, and the noise PSD is suppressed accordingly. In tight-locking condition the frequency noise PSD is efficiently reduced up to a Fourier frequency of ~500 kHz corresponding to the servo-loop control bandwidth. For frequencies lower than 100 kHz, due to the mild slope of the gas discriminator, the frequency-noise PSD is buried beneath the RIN level. Figure 3 (left axis) also reports the linewidth calculated from the measured PSD by means of the β-line method [21], for different values of the integration bandwidth (different observation times). At 1-ms observation time, the slow-lock calculated linewidth is ~1 MHz (gray

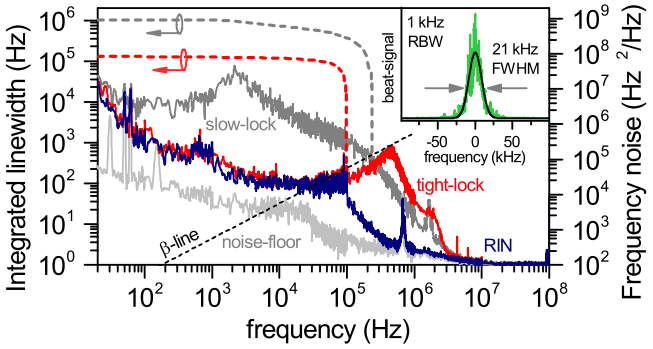

Fig. 3. Right axis: frequency noise PSD of the QCL laser in slow-lock (dark-gray line) and in phase-locked (red line) conditions together with the RIN contribution (blue), the noise floor (gray), and the β-line, $8\ln 2/\pi^2 f$ (black). Left axis: calculated emission linewidth versus integration bandwidth. Inset: beat signal (green line) between the DFG-comb and a narrow-linewidth laser at 8.6 μm, together with its Gaussian fit (black line).

dashed line of Fig. 3), in good agreement with the measured width of the QCL-comb beating signal at 1 kHz RBW. In tight-locking conditions, the integrated value of ~130 kHz (red dashed line of Fig. 3), entirely due to the RIN contribution, fixes an upper limit for the QCL linewidth. The ultimate value for the tight-locked QCL linewidth is set by the comb jitter. Exploiting the same QCL, narrowed to a 4-kHz linewidth by optical feedback-locking to an high-finesse *V*-shaped cavity [20], we measured for the RF-locked DFG-comb tooth a linewidth of ~21 kHz (inset of Fig. 3). Relying on the good phase-noise performances of the system, a final value very close to this limit can be foreseen for the QCL in tight-locking conditions [11].

In order to test the system in terms of resolution and sensitivity, we performed Doppler broadened spectroscopy of N_2O at 8.6 μm in a 10-cm-long gas cell (see Fig. 1). Figure 4 shows the transmission spectrum of the N_2O at a pressure of 8 mbar (800 Pa), resulting from a 180-kHz-wide Rb-referenced scan of f_{rep}, corresponding to an optical frequency tuning of 0.9 cm^{-1} (0.05 cm^{-1}/min frequency scan speed), sufficiently wide to precisely identify different rovibrational lines. HITRAN-based prediction of the transmission peaks for the observed lines are also shown in Fig. 4 (red dots) together with their rotational assignment. The correct integer value linking f_{rep} and the optical frequency was unambiguously assessed by taking advantage of the zero value of f_0, the considerable spectral coverage of the scan and the 30-MHz accuracy given by HITRAN for most of the investigated absorption lines [22]. Without any control of the QCL power, an absorption sensitivity of the order of 10^{-4} cm^{-1}, mainly limited by unwanted etalon effects, is achieved, as demonstrated by the inset of Fig. 4 showing a well resolved doublet with a fractional absorption of 2%.

Figure 5(a) shows the transmission profile, averaged over five consecutive scans, of the N_2O $P(8)$-*e* rovibrational line at a pressure of 1000 Pa resulting from a 1.38-GHz laser scan, together with its least squares fitting to a Voigt (b) and Galatry (c) profiles. As evidenced by the clear "*w*" structure in the residuals of Fig. 5(b), the

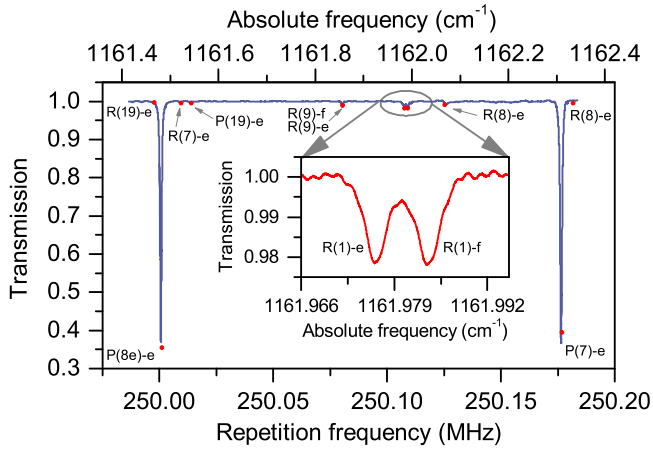

Fig. 4. N_2O transmission spectrum at 8 mbar (800 Pa) pressure, resulting from a wide scan of the comb rep-rate (bottom scale) and corresponding QCL absolute frequency (top scale). Red dots: HITRAN calculated absorption-peaks fin correspondence of our experimental conditions. Inset: detail of the $R(1)$-*e*–$R(1)$-*f* doublet with a 2% peak fractional absorption.

Voigt profile fails to reproduce the measured spectrum, owing to the occurrence of line-narrowing mechanisms. Indeed, taking into account the Dicke-narrowing effect, namely by using the Galatry profile, better results are obtained. In this case, the analysis of residuals, see Fig. 5(c), shows the absence of any systematic error apart from the unwanted etalon effects. The small absorption signature of the N_2O $R(19)$-*e* line is also revealed thanks to a signal-to-noise ratio (SNR) as high as 1400. We also performed several acquisitions of the same transition at different N_2O pressure. Figure 5(d) shows an example of the transmission profiles varying the pressure in the range from 55 to 1000 Pa (at a temperature of 296 K). A linear fit of the retrieved line-center frequencies as a function of the gas pressure allowed us to determine a pressure shifting parameter of –99(14)Hz/Pa($-3.3(5)\times10^{-4}$ cm^{-1}/atm, as well as to extrapolate the zero-pressure value of the center frequency, which resulted to be 1161.4792366(3) cm^{-1} (corresponding to a relative precision of 3×10^{-10}). This value deviates from the one of the HITRAN database by 2.6×10^{-5} cm^{-1}, well within the

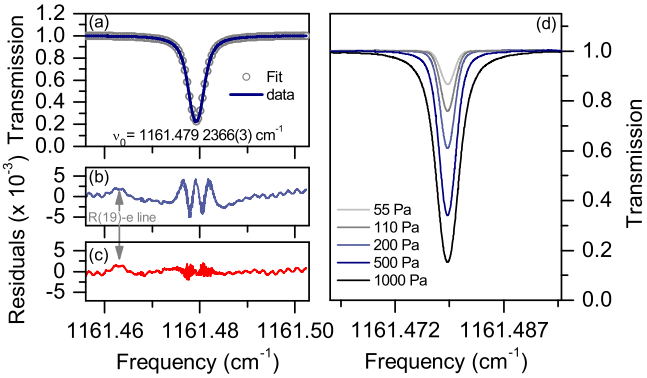

Fig. 5. (a) Averaged transmission profile (five scans) of the $P(8)$-*e* rotovibrational line of N_2O. Residuals of the (b) Voigt and (c) Galatry fits. (d) Transmission profile at different N_2O pressures.

HITRAN accuracy, and results to be 2 orders of magnitude more precise. The statistical uncertainty on the extrapolated zero-pressure value of the line-center frequency is mostly limited by the SNR of the recorded spectra and by the pressure-dependent repeatability of the line-center frequency retrievals. On the other hand, the main source of systematical deviation is the pressure reading (whose contribute amounts to 6×10^{-10}); other sources, including the electronic detection chain bandwidth [23] and the RF-standard accuracy are negligible, being at the 2×10^{-12} level.

In conclusion, we demonstrated effective phase-locking of a 8.6-μm QCL to a mid-IR optical frequency comb. Frequency- and phase-noise measurements attest a shrinking of the QCL emission linewidth from ~1 MHz to the measured ~21 kHz DFG-comb line width. High-resolution spectroscopy of N_2O molecule have also been performed demonstrating a very wide tunability (~1.4 GHz), a SNR of 1400 and a relative frequency precision of 3×10^{-10}.

The authors acknowledge financial support from the Italian Ministry of University and Research, FIRB project no. RBFR1006TZ.

References

1. J. Faist, F. Capasso, D. L. Sivco, C. Sirtori, A. L. Hutchinson, and A. Y. Cho, Science **264**, 553 (1994).
2. S. Kumar, C. W. I. Chan, Q. Hu, and J. L. Reno, Nat. Phys. **7**, 166 (2011).
3. R. M. Williams, J. F. Kelly, J. S. Hartman, S. W. Sharpe, M. S. Taubman, J. L. Hall, F. Capasso, C. Gmachl, D. L. Sivco, J. N. Baillargeon, and A. Y. Cho, Opt. Lett. **24**, 1844 (1999).
4. G. Maisons, P. Gorrotxategi-Carbajo, M. Carras, and D. Romanini, Opt. Lett. **35**, 3607 (2010).
5. F. Cappelli, I. Galli, S. Borri, G. Giusfredi, P. Cancio, D. Mazzotti, A. Montori, N. Akikusa, M. Yamanishi, S. Bartalini, and P. De Natale, Opt. Lett. **37**, 4811 (2012).
6. L. Tombez, S. Schilt, D. Hofstetter, and T. Südmeyer, Opt. Lett. **38**, 5079 (2013).
7. S. Bartalini, P. Cancio, G. Giusfredi, D. Mazzotti, P. De Natale, S. Borri, I. Galli, T. Leveque, and L. Gianfrani, Opt. Lett. **32**, 988 (2007).
8. S. Barbieri, M. Ravaro, P. Gellie, G. Santarelli, C. Manquest, C. Sirtori, S. P. Khanna, H. Linfield, and A. G. Davies, Nat. Photonics **5**, 306 (2011).
9. S. Borri, I. Galli, F. Cappelli, A. Bismuto, S. Bartalini, P. Cancio, G. Giusfredi, D. Mazzotti, J. Faist, and P. De Natale, Opt. Lett. **37**, 1011 (2012).
10. L. Consolino, A. Taschin, P. Bartolini, S. Bartalini, P. Cancio, A. Tredicucci, H. E. Beere, D. A. Ritchie, R. Torre, M. S. Vitiello, and P. De Natale, Nat. Commun. **3**, 1040 (2012).
11. A. A. Mills, D. Gatti, J. Jiang, C. Mohr, W. Mefford, L. Gianfrani, M. Fermann, I. Hartl, and M. Marangoni, Opt. Lett. **37**, 4083 (2012).
12. I. Galli, S. Bartalini, P. Cancio, F. Cappelli, G. Giusfredi, D. Mazzotti, N. Akikusa, M. Yamanishi, and P. De Natale, Opt. Lett. **39**, 5050 (2014).
13. A. Gambetta, D. Gatti, A. Castrillo, G. Galzerano, P. Laporta, L. Gianfrani, and M. Marangoni, Appl. Phys. Lett. **99**, 251107 (2011).
14. S. A. Diddams, J. Opt. Soc. Am. B **27**, B51 (2010).
15. T. Udem, R. Holzwarth, and T. W. Hänsch, Nature **416**, 233 (2002).
16. A. Schliesser, N. Picque, and T. W. Hänsch, Nat. Photonics **6**, 440 (2012).
17. A. Gambetta, N. Coluccelli, M. Cassinerio, D. Gatti, P. Laporta, G. Galzerano, and M. Marangoni, Opt. Lett. **38**, 1155 (2013).
18. V. I. Perevalov, S. A. Tashkun, R. V. Kochanov, A.-W. Liu, and A. Campargue, J. Quant. Spectrosc. Radiat. Transfer **113**, 1004 (2012).
19. F. L. Walls and A. E. Wainwright, IEEE Trans. Instrum. Meas. **24**, 15 (1975).
20. E. Fasci, N. Coluccelli, M. Cassinerio, A. Gambetta, L. Hilico, L. Gianfrani, P. Laporta, A. Castrillo, and G. Galzerano, Opt. Lett. **39**, 4946 (2014).
21. G. Di Domenico, S. Schilt, and P. Thomann, Appl. Opt. **49**, 4801 (2010).
22. R. A. Toth, J. Opt. Soc. Am. B **3**, 1263 (1986).
23. F. Rohart, S. Mejri, P. L. T. Sow, S. K. Tokunaga, C. Chardonnet, B. Darquié, H. Dinesan, E. Fasci, A. Castrillo, L. Gianfrani, and C. Daussy, Phys. Rev. A **90**, 042506 (2014).